

A Modified 3 D Space Vector based PWM Method for Four-Leg VSI Fed Asymmetrical Two-Phase Induction Motor drive using Vector Control

Dr. Heli Amit Shah

Electrical Engineering, Babaria Institute of Technology, Vadodara, Gujarat.

Abstract — This paper presents a novel three-dimensional space vector PWM method for two-phase four-leg voltage source inverter and its realization for asymmetrical two-phase induction motor drive. A general model suitable for Indirect Rotor-Field-Oriented Control (IRFOC) system of the two-phase induction machines used in this technique. The asymmetry due to unequal resistances and inductances of auxiliary and main windings is taken care of by introducing an appropriated factor k . In the mathematical model the machine main and auxiliary winding are represented in the stationary reference frame. The two phase voltages are obtained by tapping the output from terminal pairs ab and cd . The three dimensional space vector modulation without null vector is used to generate the switching signals for the inverter. Unlike the conventional Space Vector Modulation (SVM) technique, in this method the NULL vectors are eliminated and the gating signals are generated using only the non-zero active vectors. Due to this the number of transitions in a switching period is reduced. This technique reduces the switching losses in the inverter. The simulation results obtained validate the algorithm used.

Keywords: 3 D SVM, Null Vector, 2 \emptyset Induction motor, 4 – Leg VSI, Vector Control

I. INTRODUCTION

In recent years, asymmetrical two-phase induction motor (2 \emptyset I.M.) have been extensively used in low power applications [1]-[5] such as pumps, drill, compressor etc. A three-leg voltage source inverter (VSI) fed vector and scalar controlled asymmetrical 2 \emptyset I.M. drives have been widely developed. The most popular topology is the three-leg VSI drives using pulse width modulation (PWM) control [6]-[9]. Based on this principle, the auxiliary and main winding voltages of asymmetrical 2 \emptyset I.M.s are required to have a phase difference of 90° and independent magnitude with respect to each other. The voltage magnitude relationship of the two-phase depends on the turn ratio of windings. The auxiliary winding phase voltage is higher than the main winding phase voltage of the machine.

The sinusoidal PWM control strategy is used in [8, 9]. A simple scalar volts/hertz control is used to generate the reference voltages. The three leg VSI is used as Power converter. Though it offers good steady state and dynamic performances, this topology suffers from neutral point balance. In paper [1] the four-leg inverter with SPWM technique is used. This technique has less DC bus voltage utilization compared to the space vector pulse width modulation technique.

In this paper a novel three dimensional space vector pulse width modulation technique (3D SVPWM) without the null vector is proposed. The proposed control algorithm can generate unbalanced two-phase output voltage waveforms with independently adjustable amplitudes on each output phase.

Section II describes the mathematical model of the asymmetrical 2 \emptyset I.M. Section III and IV present indirect rotor field oriented control characteristics and a four-leg VSI topology with proposed switching technique, respectively. Simulation results are discussed in Section V.

II. MATHEMATICAL MODEL OF ASYMMETRICAL 2 \emptyset I.M.

The d - q axes equivalent circuits of an asymmetrical 2 \emptyset I.M. in stationary reference frame is shown in Fig. 1 (a & b). The complete mathematical model equation of machine in the stationary reference frame is represented as follows:

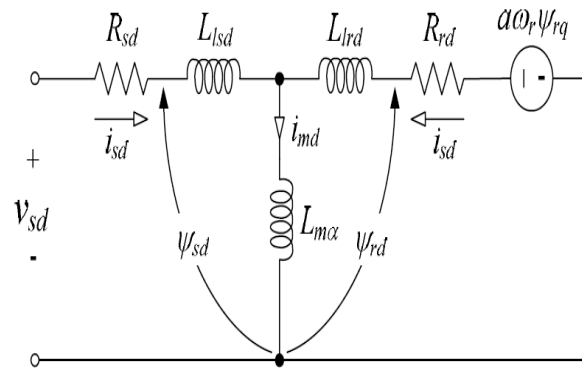


Fig. 1(a): d-axis equivalent circuit

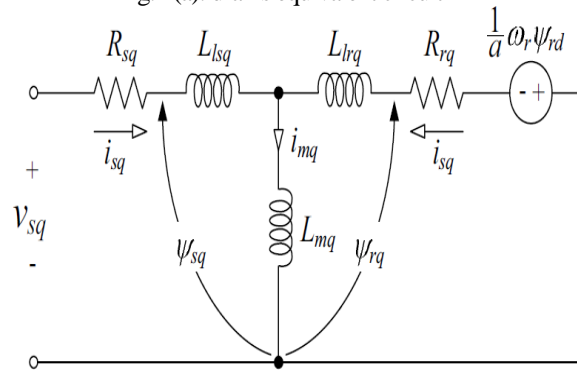


Fig. 1(b): q-axis equivalent circuit

$$v_{sd} = R_{sd}i_{sd} + \frac{d\phi_{sd}}{dt} \quad (1)$$

$$v_{sq} = R_{sq}i_{sq} + \frac{d\phi_{sq}}{dt} \quad (2)$$

$$R_r i_{rd} + \frac{d\phi_{rd}}{dt} - \omega \phi_{rq} = 0 \quad (3)$$

$$R_r i_{rq} + \frac{d\phi_{rq}}{dt} - \omega \phi_{rd} = 0 \quad (4)$$

The stator and rotor flux linkage components are given by

$$\phi_{sd} = L_{sd}i_{sd} + M_{srd}i_{rd} \quad (5)$$

$$\phi_{sq} = L_{sq}i_{sq} + M_{srq}i_{rq} \quad (6)$$

$$\phi_{rd} = L_r i_{rd} + M_{srd}i_{sd} \quad (7)$$

$$\phi_{rq} = L_r i_{rq} + M_{srq}i_{sq} \quad (8)$$

where v_{sd} , v_{sq} are the stator voltages, i_{sd} , i_{sq} , i_{rd} , i_{rq} are the stator and rotor currents, R_{sd} , R_{sq} , R_{rd} , R_{rq} are the stator and rotor resistances, L_{sd} , L_{sq} , L_{rd} , L_{rq} are the stator and rotor self inductances, M_{srd} , M_{srq} are the mutual inductances, ω is the rotor angular speed (expressed in electrical rad/s), and d , q subscripts used to represent auxiliary and main windings quantities, respectively. The mechanical equation is given by (9) and the electromagnetic torque is expressed by (10).

$$J \frac{d\omega}{dt} + f_r \omega = n_p (T_e - T_l) \quad (9)$$

$$T_e = n_p (M_{srq}i_{sq}i_{rd} - M_{srd}i_{sd}i_{rq}) \quad (10)$$

In order to assure the control and the parameter estimation, the 2 ϕ I.M. model should be represented in state space frame as given by (11). The 2 ϕ I.M. state space model in a stationary reference frame is given by (12).

$$\frac{d[X]}{dt} = [A][X] + [B][U] \quad (11)$$

$$\frac{d}{dt} \begin{bmatrix} i_{sd} \\ i_{rq} \\ \phi_{rd} \\ \phi_{rq} \end{bmatrix} = \begin{bmatrix} \frac{1}{\sigma_d \tau_{sd}} - \frac{1 - \sigma_d}{\sigma_d \tau_r} & 0 & \frac{1 - \sigma_d}{\sigma_d M_{srd} \tau_r} & \frac{1 - \sigma_d}{\sigma_d M_{srd}} \omega \\ 0 & -\frac{1}{\sigma_q \tau_{sq}} - \frac{1 - \sigma_q}{\sigma_q \tau_r} & \frac{1 - \sigma_q}{\sigma_q M_{srq}} \omega & \frac{1 - \sigma_q}{\sigma_q M_{srq} \tau_r} \\ \frac{M_{srd}}{\tau_r} & 0 & -\frac{1}{\tau_r} & -\omega \\ 0 & \frac{M_{srq}}{\tau_r} & \omega & -\frac{1}{\tau_r} \end{bmatrix} \begin{bmatrix} i_{sd} \\ i_{rq} \\ \phi_{rd} \\ \phi_{rq} \end{bmatrix} \quad (12)$$

$$+ \begin{bmatrix} \frac{1}{\sigma_d L_{sd}} & 0 \\ 0 & \frac{1}{\sigma_q L_{sq}} \\ 0 & 0 \\ 0 & 0 \end{bmatrix} \begin{bmatrix} v_{sd} \\ v_{rq} \\ 0 \\ 0 \end{bmatrix}$$

In which

$$\sigma_d = 1 - \frac{M_{srd}^2}{L_{sd} L_r} \quad (13)$$

$$\sigma_q = 1 - \frac{M_{srq}^2}{L_{sq} L_r} \quad (14)$$

$$\tau_{sd} = \frac{L_{sd}}{R_{sd}} \quad (15)$$

$$\tau_{sq} = \frac{L_{sq}}{R_{sq}} \quad (16)$$

$$\tau_r = \frac{L_r}{R_r} \quad (17)$$

III. INDIRECT ROTOR FIELD ORIENTED CONTROL

Note that (1) - (10) are general equations for the two-phase machine. They may represent either a symmetrical or an asymmetrical model, it can be seen from (10) that the machine produces torque oscillations if the d and q are balanced. The term balanced denotes that the variables d and q are sinusoidally phase shifted by 90° and with the same amplitude. This asymmetry is due to the unequal resistances and inductances of the main and auxiliary windings. However, to use the field orientation control of unbalanced two-phase induction motor, the asymmetry must be eliminated using an appropriate variable changing as presented in [10]:

$$i_{sd}^s = i_{sd1}^s \quad (18)$$

$$i_{sq}^s = k i_{sq1}^s \quad (19)$$

$$\text{Where, } k = \frac{M_{srd}}{M_{srq}} \quad (20)$$

By substituting the variables i_{sd} and i_{sq} for the auxiliary variables i_{sd1} and i_{sq1} into (10), the torque can be expressed by:

$$T_e = \frac{n_p}{L_r} M_{srd} (i_{sq1}^s \phi_{rd} - i_{sd1}^s \phi_{rq}) \quad (21)$$

The new expression of the electromagnetic torque is similar to that of a symmetrical machine. The relationship between rotor-flux components and stator currents in the stationary reference frame are deduced from (3), (4), (7), (8), (18) and (19) equations.

$$\frac{d\phi_{rd}}{dt} = \frac{M_{srd}}{\tau_r} i_{sd1}^s - \frac{1}{\tau_r} \phi_{rd} - \omega \phi_{rq} \quad (22)$$

$$\frac{d\phi_{rq}}{dt} = \frac{M_{srd}}{\tau_r} i_{sq1}^s - \frac{1}{\tau_r} \phi_{rq} - \omega \phi_{rd} \quad (23)$$

The vector model is defined from (22) and (23) by rearranging the variables in the vector form. If this vector model is written for an arbitrary reference frame (denoted by superscript a), which is δ_a rad away from phase d of the stator, then

$$\frac{d\phi_r^a}{dt} = -\frac{1}{\tau_r} \phi_r^a - j(\omega_a - \omega) \phi_r^a + \frac{M_{srd}}{\tau_r} i_{s1}^a \quad (24)$$

And ω_a is the speed of the arbitrary reference frame. The variables in the arbitrary reference frame are calculated from the variables in the stator reference frame through the following equations:

$$\phi_r^a = \phi_{rd}^a + j\phi_{rq}^a \quad (25)$$

$$i_{s1}^a = i_{sd1}^a + ji_{sq1}^a \quad (26)$$

Based on the vector model given by (21) and (24) it is possible to apply the field oriented principles to control the rotor flux and electromagnetic torque of two-phase machine. For that, the rotor flux reference frame (denoted by the superscript rf) is chosen and, consequently, which means orienting the reference frame along the rotor flux. By doing so the quadrature component becomes zero.

$$\phi_{rd}^{rf} = \phi_r^a \quad (27)$$

$$\phi_{rq}^{rf} = 0 \quad (28)$$

Then torque and flux-current equations in the rotor-flux reference frame can be obtained from (24),

$$\frac{M_{srd}}{\tau_r} i_{sd1}^{rf} = \frac{\phi_r}{\tau_r} + \frac{d\phi_r}{dt} \quad (29)$$

$$\frac{M_{srd}}{\tau_r} i_{sq1}^{rf} = \omega_{s1} \phi_r \quad (30)$$

Using (21), the expression for the torque can be calculated by:

$$T_e = \frac{n_p}{L_r} M_{srd} i_{sq1}^{rf} \phi_r \quad (31)$$

Where $\omega_{sl} = \omega_s - \omega$ is the slip frequency, ω_s and δ_{rf} are respectively the frequency and the position of the rotor flux vector. Then, i_{sd1}^{rf} controls the rotor flux and i_{sq1}^{rf} controls the electromagnetic torque. Fig.2 shows the block diagram of indirect rotor-field-oriented control scheme, which has been adapted for the two-phase machine. In this diagram T_e^* and ϕ_r^* represent the reference electromagnetic torque and amplitude of the rotor flux, respectively. Block performs the coordinate transformation from the reference frame aligned along with the rotor-flux vector to the stationary reference frame. Furthermore, i_{sd}^* and i_{sq}^* represent the reference currents supplied to the PI stator current controllers, which must be injected on the machine windings. It is seen that the two current controllers provide control voltages V_{sd} and V_{sq} . These voltages are used to generate the reference vector which is used in the proposed switching technique. Speed sensor gives information about rotor angular speed.

IV. PROPOSED SWITCHING TECHNIQUE

Fig. 2 shows the block diagram of the closed loop control of two phase induction motor for 4 leg VSI. Speed control is done using indirect rotor flux oriented control method. Switching pulses for four leg VSI are generated using modified 3D-SVPWM method. With the indirect rotor flux oriented control of induction motor we get the stationary voltages in the synchronous reference frame. The same voltages are converted in to α - β frame and then into stationary reference frame for prism and tetrahedron identification respectively. The asymmetrical 2ϕ I.M. is connected to 4 leg VSI as shown in Fig. 3. It is composed of four legs with two devices on each leg.

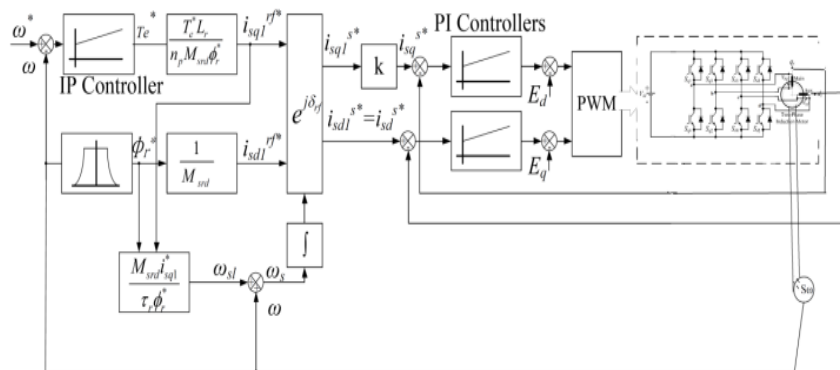


Fig. 2: Block Diagram of the 2ϕ I.M. with proposed method

The 3D-SVPWM without considering null vector (proposed method) is implemented in the following sequence: (i) Identification of prism; (ii) Identification of tetrahedrons; (iii) Duty cycle calculation; (iv) Generation of PWM sequence for the switches. The first two steps for implementation of 3D-SVPWM, like identification of prism and tetrahedrons are well elaborated in [4]. The most important step in 3D-SVPWM is to calculate the duty cycle and to translate the information into four PWM waveforms for the given sequencing scheme.

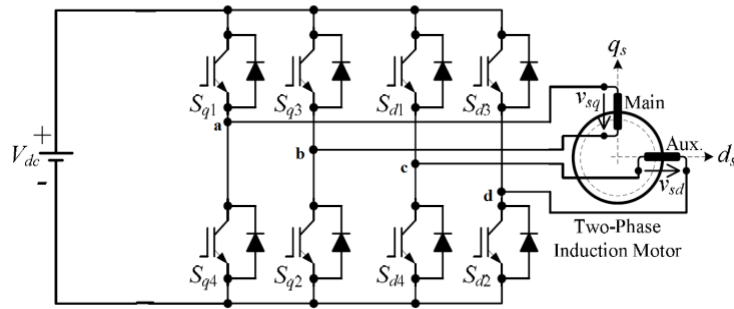


Fig. 3: Two Phase 4 Leg VSI

A. Prism Identification

The prism identification is very similar to the sector identification for 2-D SVM. Based on the projections of the reference vector on the α - β plane, v_α and v_β , six prisms in the 3-D space can be identified and numbered as Prisms I through VI. Within the selected prism, there are six non-zero switching state vectors and two zero switching state vectors which are eliminated in proposed technique. Fig. 4 shows the physical positions of the switching state vectors in 0 - α - β coordinate system.

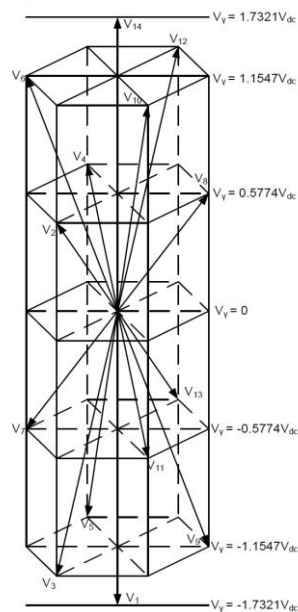


Fig. 4: Physical Position of Switching State Vector

The identification of prism is based on the value of the switching vectors expressed in 0 - α - β reference frame. An algorithm for prism identification is explained with the help of a flowchart. Fig. 5 shows the logic flow in prism identification.

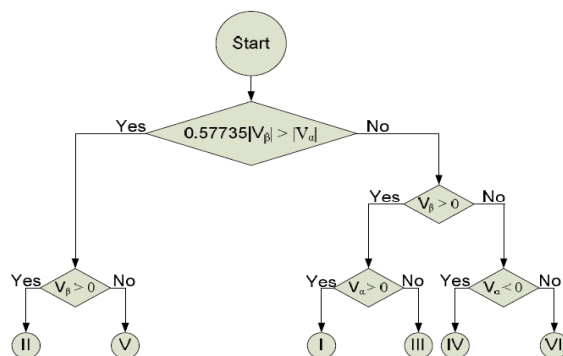


Fig. 5: Sequence of Operations in Prism Identification

B. Tetrahedron Identification

Once the prism information is obtained the next step is to identify the tetrahedron in which the reference vector is present. To do this each prism is further subdivided into four tetrahedrons - thus leading to a total of 24 tetrahedrons. Each tetrahedron is formed by

three non-zero switching state vectors and two zero switching state vectors. The line-to-neutral voltage polarities produced by each non zero switching state vectors are indicated as '+' or '-' or '0'. It is important to notice that within each tetrahedron, all the non zero switching state vectors produce non-conflicting line-to-neutral voltages, and thus they are adjacent vectors. These tetrahedrons could be identified based on the sign of required phase voltages at the output of the inverter [4].

C. Duty cycle Calculation and Pulse Generation

The computation of the duty cycles is based on calculation of geometric projection of the reference vector along the three non-zero switching state vectors which form the edges of the given tetrahedron at a given instant. For each tetrahedron we can find a 3x3 projection matrix: S_t . The reference vector in 0- α - β reference frame at any given time is denoted by a 3x1 column matrix S_r . Then at any given instant, the duty cycle matrix D can be computed from the simple matrix equation (32).

$$D = \begin{bmatrix} d_1 \\ d_2 \\ d_3 \end{bmatrix} = S_t^{-1} * S_r \quad (32)$$

As the null vector is eliminated the duration for each switching period varies. The switching period is determined by $(d_1 + d_2 + d_3) * T_s$ where T_s is the sampling period if the null vectors were considered. This results in variable switching frequency operation. Though the frequency of operation is not constant it varies over a small range only. This is evident from the plot of $(d_1 + d_2 + d_3)$ as a function of time as shown in Fig. 6. When reference vector is pure sine wave the switching frequency varies from $\frac{1}{0.7T_s}$ to $\frac{1}{0.6T_s}$ i.e. 14 kHz to 16 kHz for a sampling frequency of 20 kHz.

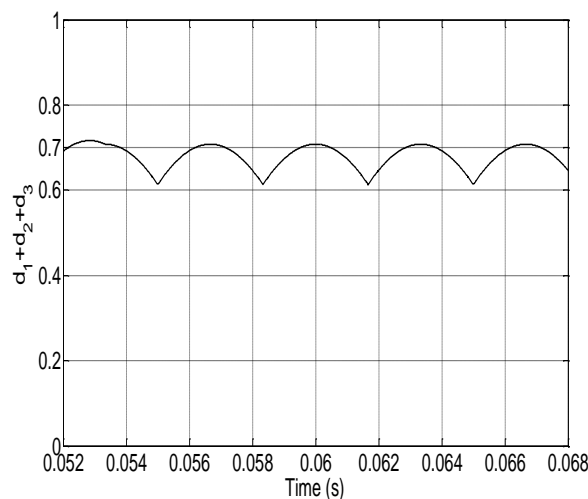


Fig. 6: Plot of $(d_1+d_2+d_3)$ with Reference vector derived from balanced three phase sinusoidal voltages

The next step is to choose an appropriate switching scheme and to generate the four PWM pulses for the top switches of the inverter. The three duty-cycle values d_1 , d_2 and d_3 are already known prior to this step. The PWM pulses are generated by comparing the four signals X_1 , X_2 , X_3 , and X_4 with a triangular waveform of switching frequency equals to the sampling frequency of the modulator, where sampling frequency of modulator is given by $(d_1+d_2+d_3) * T_s$. Let X_1 , X_2 , X_3 and X_4 are the four signals calculated from the duty cycles d_1 , d_2 , and d_3 as given in the matrix equation (33) – (35).

$$X_t = \begin{bmatrix} X_2 \\ X_3 \end{bmatrix} = 2 * A_t \begin{bmatrix} \frac{d_1}{2} \\ \frac{d_1}{2} + \frac{d_2}{2} \end{bmatrix} \quad (33)$$

$$X_4 = 1 \quad (34)$$

$$X_1 = 0 \quad (35)$$

In (33), A_t is the peak value of the triangular waveform. The period of this waveform is $(d_1+d_2+d_3) * T_s$, which decides the switching frequency of the inverter. The relation between the elements of matrix X_t and the switching signals S_a , S_b , S_c , and S_f would be different for different tetrahedrons. The assignment of the pulses generated by the comparator is given in [4]. Fig. 7 shows the set of signals derived for tetrahedron formed by the switching vectors V_2 , V_6 and V_7 . It is seen that the switching signals S_a and S_f not undergo any transition during one switching cycle. This is the major advantage of this switching scheme. It reduces the number of switching in one fundamental period thus reducing the switching losses.

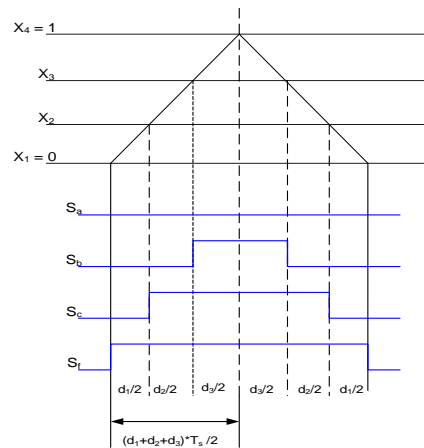


Fig. 7: Principle of PWM waveform Generation

Using the proposed method the open loop speed control of 2-ph induction motor is implemented MATLAB/SIMULINK and the results are presented in the following section.

V. SIMULATION RESULTS

The modeling of an asymmetrical 2Ø I.M. in this paper has been developed in Matlab/Simulink environment. The four leg inverter topology shown in Fig. 3 is used for simulation studies. The motor parameters used for the simulation are listed in Table I. To demonstrate feasibility of the proposed closed loop SVPWM algorithm for the two-phase four-leg VSI, the inverter is supplied a constant dc-link voltage at 500 V.

The ratings of the asymmetrical 2Ø I.M are 1/2 hp, 220 V, 50 Hz. Fig. 8 shows the simulated waveforms for steady-state output voltages v_{sd} , v_{sq} of the unbalanced two-phase four-leg VSI when the asymmetrical 2Ø I.M. utilizing the proposed method. It can be seen that the output voltages are identical in amplitude at 50 Hz, while the voltages are displaced at 90°.

TABLE I: SIMULATION PARAMETERS FOR ASYMMETRICAL 2Ø I.M.

$R_{sd} = 2.4\Omega$	$L_{sd} = 0.0909H$	$M_{srd} = 0.0829H$
$R_{sq} = 5.66\Omega$	$L_{sq} = 0.115H$	$M_{srq} = 0.099H$
$R_r = 6.161\Omega$	$L_r = 0.0915H$	$J = 2.63 \text{ e-}4 \text{ kg-m}^2$
$n_p = 2$	$f_r = 2.026\text{e-}4 \text{ Nms/rad}$	$Tl = 5 \text{ N/m}$

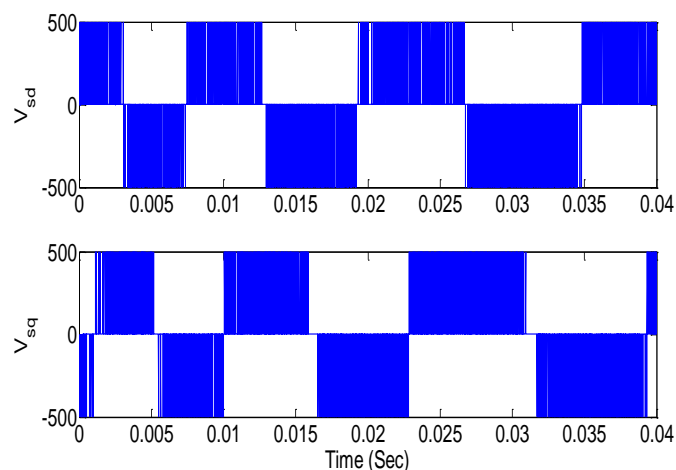


Fig. 8: Two-phase voltage waveform of the auxiliary and the main winding. v_{sd} , v_{sq}

The simulations have been performed for a starting at no load from zero to rated speed $\omega = 250 \text{ rad/s}$ with prescribed behavior, linear increase of speed for one and a half second as shown in Fig.9, presents command and actual speed. Fig. 9 represents the soft start of motor with no load.

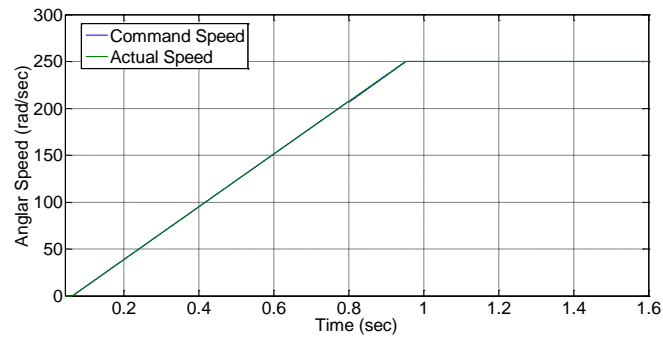


Fig. 9: Reference and Real angular rotor speed

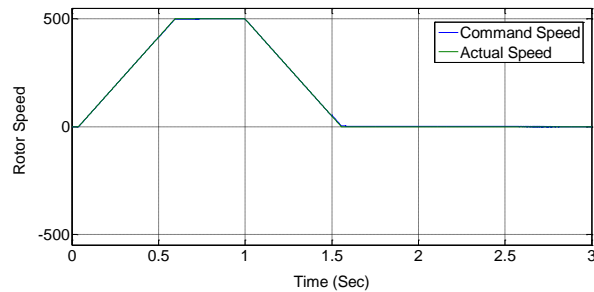


Fig. 10: Command and Actual Rotor Speed

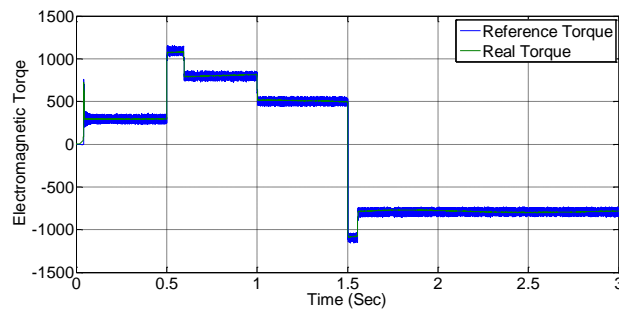


Fig. 11: Reference and Real Electromagnetic Torque

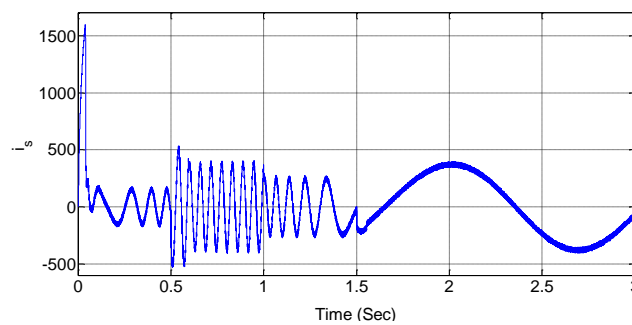


Fig. 12: Stator Current with change in speed and torque

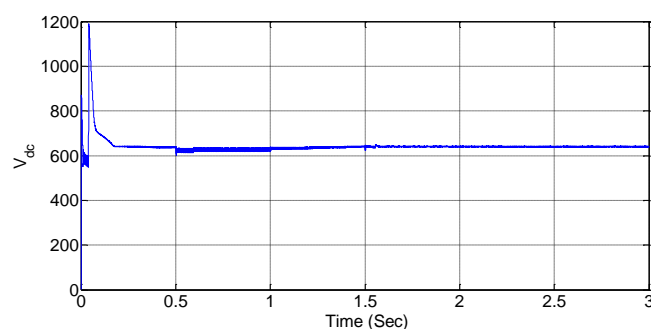


Fig. 13: DC Bus Voltage Variation

Fig. 10 depicts the change in rotor angular speed of motor. At time $t = 0$ s, the speed set point is 500 rpm. The speed follows precisely the acceleration ramp. At $t = 0.5$ s, the full load torque is applied to the motor shaft while the motor speed is still ramping to its final value. This forces the electromagnetic torque to increase to the user-defined maximum value (1200 N.m) and then to stabilize at 820 N.m as shown in fig. (11). Once the speed ramping is completed and the motor has reached 500 rpm.

At $t = 1$ s, the speed set point is changed to 0 rpm. The speed decreases down to 0 rpm by following precisely the deceleration ramp even though the mechanical load is inverted abruptly, passing from 792 N.m to - 792 N.m, at $t = 1.5$ s. Shortly after, the motor speed stabilizes at 0 rpm.

Finally, the DC bus voltage is regulated during the whole simulation period as shown in fig. (13).

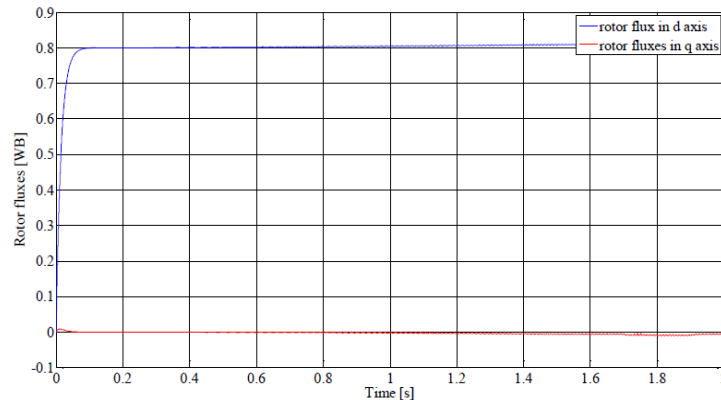


Fig. 14: Rotor Fluxes in Synchronous Reference Frame

From Fig.14, the reference d-axis rotor flux is kept constant at 0.8Wb while the q-axis rotor flux remains null, so it is clear that the rotor fluxes is aligned with the d-axis. As shown in the simulation, the proposed control algorithm has an improved and robust performance.

VI. CONCLUSION

In this paper the modified 3D-SVPWM method for two-phase four leg VSI fed asymmetrical 2ϕ I.M. is proposed. The control strategy for two-phase operation has been developed to synthesize unbalanced two-phase output voltage waveforms with closed loop indirect rotor flux oriented control. The proposed SVPWM method can generate two phase output voltages with independently adjustable magnitudes in two output phases. The proposed PWM scheme allows the four-leg VSI to feed sinusoidal output orthogonal voltages for asymmetrical 2ϕ I.M. which is unbalanced two-phase load. The simulation results confirm the feasibility of the developed control scheme for the two-phase four-leg VSI drive system.

REFERENCES

- [1] A. M. Hava, R. J. Kerkman, and T. A. Lipo, "Carrier- Based PWM-VSI Over modulation Strategies: Analysis, Comparison, and Design", *IEEE Transactions on Power Electronics*, vol. 13, no. 4, pp. 674-689, July 1998.
- [2] F. Blaabjerg, F. Lugeanu, K. Skaug, and M. Tonnes, "Two-Phase Induction Motor Drives", *IEEE Industry Applications Magazine*, vol. 10, pp. 24-32, July/August2004.
- [3] E. Muljadi, Y. Zhao, T. H. Liu, and T. A. Lipo, "Adjustable ac Capacitor for a Single-Phase Induction Motor", *IEEE Transactions on Industrial Electronics*, vol.29, no. 3, pp. 479-485, 1993.
- [4] Heli Golwala, R. Chudamani, "Simulation of Three-phase Four-wire Shunt Active Power Filter using Novel Switching Technique", *IEEE PEDES Conference*.
- [5] C. M. Young, C. C. Liu, C. H. Liu. "New Inverter- Driven Design and Control Method for Two-Phase Induction Motor Drives", *IEE Proceedings-Electric Power Applications*, volume 143, no. 6, pp. 458-466, (1996).
- [6] M. B. de R. Correa C. B. Jacobina, A. M. N. Lima, E. R. C. da Silva. "A Three-Leg Voltage Source Inverter for Two-Phase AC Motor Drive Systems", *IEEE Transaction Power Electronics*, volume 17, no. 4, pp. 517-523, (2002).
- [7] V. Kinnares, Ch. Charumit. "Modulating Functions of Space Vector PWM for Three-Leg VSI-Fed Unbalanced Two-Phase Induction Motors", *IEEE Transaction Power Electronics*, volume 24, no. 4, pp. 1135-1139, (2009).
- [8] Do-Hyun. "PWM Methods for Two-Phase Inverters", *IEEE Industry Applications Magazine*, volume 13, pp. 50-61, (2007).
- [9] Ch. Charumit, V. Kinnares, "Carrier-Based Unbalanced Phase Voltage Space Vector PWM Strategy for Asymmetrical Parameter Type Two-Phase Induction Motor Drives", *Electric Power System Research*, volume 79, pp. 1127-1135, (2009).
- [10] M.B.R. Corrêa, C.B. Jacobina, E.R.C. Da Silva, A.M.N. Lima.: Vector control strategies for single-phase induction motor drive systems, In: *IEEE Transaction on Industrial Electronics*, October 2004, vol. 51, pp. 1073 – 1080.